Food Research International 242 (2026) 119939

Contents lists available at ScienceDirect

Food Research International

journal homepage: www.elsevier.com/locate/foodres

Metagenomic profiling reveals how ecological and processing drivers shape the beef microbiome from farm to fork

Asim ur Rahman [a,b], Vincenzo Valentino [a], José F. Cobo-Díaz [c], Giuseppina Sequino [a], Avelino Alvarez Ordóñez [c], Danilo Ercolini [a,b], Francesca De Filippis [a,b,d,*]

[a] Department of Agricultural Sciences, University of Naples Federico II, Via Università 100, 80055 Portici, Italy
[b] Task Force on Microbiome Studies, University of Naples Federico II, Corso Umberto I 40, 80138 Naples, Italy
[c] Department of Food Hygiene and Technology and Institute of Food Science and Technology, Universidad de León, 24071 León, Spain
[d] Institute of Biotechnology and Food Technology, Industrial University of Ho Chi Minh City, 12 Nguyen Van Bao Street, Go Vap district, Ho Chi Minh City, Viet Nam

ARTICLE INFO

Keywords:
Meat wet-aging
Meat spoilage
Food processing environments
Antimicrobial resistance genes
Biofilm formation
Bacteriophages
Food safety

ABSTRACT

Meat processing environments harbor complex microbial ecosystems that may be transferred to the final product, thus influencing product quality and safety. Several factors may affect microbiome composition, such as seasonality and sanitation procedures. In this study, we carried out a metagenomic analysis over two seasons across four beef processing facilities, following beef carcasses from farm-to-fork. The pre-maturation environment was dominated by *Corynebacterium xerosis* and *Acinetobacter johnsonii* in summer, and by *Bifidobacterium pseudolongum* and *Cutibacterium acnes* in winter, whereas meat maturation environments were colonized by a specialized lactic acid bacterial community. The long-term maturation stage was led by *Carnobacterium divergens* and *Carnobacterium maltaromaticum*, whereas *Pseudolactococcus carnosus* and *Pseudolactococcus paracarnosus* prevailed during the retail stage. The environmental microbiome exhibited broad metabolic potential, in contrast to the specialized, low-diversity profiles of mature meat. Routine sanitation practices did not fully remove detectable microbial DNA signatures from environmental surfaces and were associated with shifts in taxonomic and functional profiles, including a greater representation of biofilm-associated genes. We also identified a diverse phage community, and statistical modeling revealed strong negative predictive associations with *Listeria monocytogenes*, *Salmonella enterica,* and *Staphylococcus aureus*. Collectively, our findings demonstrate that the beef processing microbiome is shaped by the interaction of multiple ecological forces. Understanding these interactions provides a comprehensive framework for ecology-based strategies to improve meat quality, safety, and shelf-life.

1. Introduction

Globally, approximately 25% of all meat is lost at the production or consumer stage, resulting in significant food waste and revenue losses (Karwowska et al., 2021). The environmental impact is further exacerbated by the high consumption of water, feed, and energy, as well as methane emissions associated with animal production and meat waste decomposition (World Wildlife Fund, 2021; Poore & Nemecek, 2018; FAO, 2013). For instance, in the United States, an estimated 194,700 t of beef is discarded annually due to spoilage, equivalent to the waste of up to 780,000 cattle and the resources used in their production (Ramanathan et al., 2022). These losses highlight that understanding and controlling microbial dynamics in commercial meat processing is not only a matter of quality control, but also a fundamental challenge for global food security and environmental sustainability.

It is well documented that the food-processing environment may be an active source of contamination that shapes the microbial structure of food products. Meat processing environments harbor a complex resident microbiome, often including biofilm-forming taxa that provide protection against sanitation procedures (De Filippis et al., 2021). Environmental taxa may be transferred to the meat, contributing to spoilage dynamics, or posing food safety risks. Previous studies have highlighted that meat industry resident communities are a rich source of spoilage (e.g., *Pseudomonas, Acinetobacter, Psychrobacter, Brochothrix,* and *Moraxella*) and pathogenic microorganisms (e.g., *Salmonella enterica* and *Listeria monocytogenes*) (De Filippis et al., 2021; Sequino et al., 2024, 2025;

* Corresponding author at: Department of Agricultural Sciences, University of Naples Federico II, Via Università 100, 80055 Portici, Italy.
E-mail address: francesca.defilippis@unina.it (F. De Filippis).

https://doi.org/10.1016/j.foodres.2026.119939
Received 5 May 2026; Received in revised form 10 June 2026; Accepted 6 July 2026
Available online 7 July 2026

Véghová et al., 2017; Yeom et al., 2024),(De Filippis et al., 2021; Sequino et al., 2024, 2025; Véghová et al., 2017; Yeom et al., 2024) showing a wide array of genes involved in spoilage-related activities or potential harms, such as biocide resistance, virulence, and antimicrobial resistance genes (Barcenilla, Cobo-Díaz, Puente, et al., 2024; Cobo-Díaz et al., 2021; Sequino et al., 2025).

Despite improvements in sequencing technologies and hygiene monitoring, the current understanding of microbial dynamics in modern meat processing chains remains fragmented. While numerous studies have relied on 16S rRNA amplicon sequencing to characterize microbial communities, only a limited number have applied whole metagenome sequencing (WMS), which provides deeper insights into both taxonomic composition and functional potential. Most existing WMS studies have focused on single processing facilities, often based on one-time sampling (Sequino et al., 2024) or within a short timeframe (Cobo-Díaz et al., 2021). In addition, several studies have been restricted to specific steps along the meat processing chain, such as slaughterhouses or butcher shop environments (Manfreda et al., 2026; Shedleur-Bourguignon et al., 2023; Xu et al., 2025). Consequently, the critical transitions shaping microbial progression from initial contamination during processing to stable communities in mature meat remain insufficiently explored, despite recent efforts to address this gap (Fernández-Trapote et al., 2026).

To bridge these knowledge gaps, this study employed a comprehensive whole metagenomic survey across four commercial beef processing chains, sampled in summer and winter, to provide a comparative view of the beef microbiome structure and functional potential across seasons and to map microbial succession along the processing chain from farm to retail. In addition, we assessed the impact of sanitation practices on microbial dynamics, sampling the same facilities before and after routine cleaning, and explored the resident bacteriophage community and its potential links with the facility microbiome. In this context, we further hypothesized that processing stage, seasonality, and sanitation practices represent key ecological drivers shaping microbiome composition and functional potential along the beef processing chain.

2. Methodology

2.1.1. Sampling strategy

Four Irish beef processing chains located in major production regions were visited during summer 2023 and winter 2024. Food-contact and non-food contact samples were collected from the farm, lairage hall, slaughter hall, chiller hall, boning hall, and retail hall, both during processing and after sanitation, by swabbing surfaces with Whirl-Pak Hydrated PolyProbe swabs (Whirl-Pak, Madison, Wisconsin, US), covering 1 m^2 for surfaces with non-standardized areas or one unit for discrete items (e.g., knives; Supplementary Table 1 and Fig. 1), following the protocol developed by Barcenilla, Cobo-Díaz, De Filippis, et al. (2024). Negative controls pools of five swabs left exposed for 1 min to the air of the processing plant (negative control–industry) or of the laboratory where samples were manipulated and DNA extracted (negative control–laboratory) were included as previously reported (Barcenilla, Cobo-Díaz, De Filippis, et al., 2024). Farm sampling was conducted on the same morning prior to slaughter. Personnel involved in sample collection wore protective coats, shoes, caps, and facial masks throughout the sampling, and changed gloves between samples to prevent cross-contamination. Swab samples were kept chilled in portable polystyrene coolers until arrival to the laboratory, where they were frozen at −80 °C. For each chain, four cattle were sequentially followed from the farm through the processing steps, with both the left and right sides of the carcasses swabbed. Furthermore, the final meat products underwent controlled wet-aging, followed by chilled storage during the retail shelf-life phase. Vacuum-packed products were maintained at 0–3 °C in a temperature-controlled cooling chamber. Long-term maturation involved aging vacuum-packed meat chunks for up to 77 days, with independent packages opened only at each sampling time point (2, 10, 22, 35, 49, and 77 days) to avoid external contamination. The retail hall was common to all four beef processing chains across both seasons. After each maturation time point, vacuum-packed meat was transported under controlled conditions (0–3 °C) to the retail facility, maintaining the cold chain throughout handling and transport. Retail phase maturation involved the slicing of 22-day matured meat into retail portions, which were further stored under vacuum for 24 days at 0–5 °C. Retail

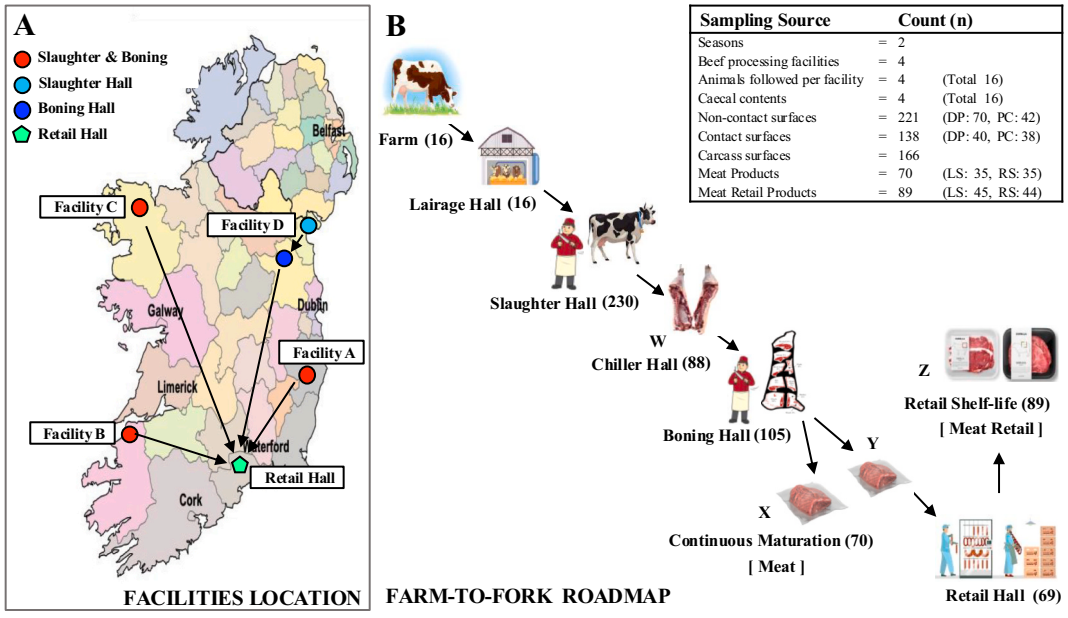

Fig. 1. Sampling locations and collection strategy. (A) Map of the selected facilities across the Republic of Ireland. Different colors correspond to the distinct processing stages conducted at each location. (B) Detailed workflow illustrating the sampling points and their direction, i.e., from farm-to-fork. Numbers in brackets represent the total number of samples from that specific processing step. W = Carcasses stored in chiller hall for 36 h at 0–3 °C; X = Wet-aged meat products sampled at 2, 10, 35, 49, and 77 days; Y = Wet-aged meat products for 22 days; Z = Retail phase meat products sampled at 0, 3, 10, 17, and 24 days. The table summarizes the sampling sources and the respective number of samples collected (n). DP = During Production; PC = Post Cleaning; LS = Left Silverside; RS = Right Silverside.

samples were collected after 0, 3, 10, 17, and 24 days, using independent sliced portions derived from the same 22-day matured meat batch to ensure replication while minimizing contamination bias.

2.1.2. DNA extraction and sequencing

Microbial cells were recovered from each swab sample (except for retail meat samples, where three independent portions were swabbed as biological replicates) in sterile phosphate-buffered saline (PBS) solution supplemented with 0.1% (*v*/v) Triton X-100 (PBS-T; 137 mM NaCl, 10 mM Na_2HPO_4, 1.8 mM KH_2PO_4, pH 7.4). The cells were detached from the swabs using a homogenizer (300 rpm, 90 s), and the suspension was centrifuged at 12,000 ×*g* for 2 min. This process was repeated twice to maximize cell recovery. The resulting pellet was washed twice with sterile PBS and stored at −80 °C until DNA extraction. DNA was extracted from the stored pellets using the MolYsis™ Complete5 Kit (Molzym, Bremen, Germany) according to the manufacturer's instructions. DNA concentration was quantified using a Qubit HS Assay (Thermo Fisher Scientific, Waltham, MA, USA). Out of 712 total extracted samples, 28 were dropped due to low DNA yields, leaving 684 samples that successfully proceeded to sequencing. All negative controls (collected both at industry level and laboratory level) did not yield high-quality library and were not sequenced. Sequencing libraries were prepared with the Nextera XT Index Kit v2 (Illumina, San Diego, CA, USA). Whole metagenome sequencing was performed on an Illumina NovaSeq 6000 platform to generate 2 × 150 bp paired-end reads. Shotgun metagenomic sequencing generated a total of 21.72 billion raw reads across the two batches of samples, collected during summer 2023 (11.23 billion reads; 33.44 M average per sample) and winter 2024 (10.49 billion reads; 30.22 M average per sample).

2.2. Bioinformatic analysis

2.2.1. Raw sequencing data pre-processing

Host sequences from the samples were removed by mapping the reads to the *Bos taurus* reference genome (Accession Number GCA_002263795.4) using the Best Match Tagger (https://www.hmpdacc.org/hmp/doc/HumanSequenceRemoval_SOP.pdf), with default options, following the Human Microbiome Project host-removal protocol adapted for *Bos taurus*. The remaining non-host microbial reads were quality-filtered using Prinseq-lite (v0.20.4) to trim low-quality reads from the 3′ ends and remove reads shorter than 60 bp (options "-trim_qual_right 5" and "-min_len 60") (Schmieder & Edwards, 2011). After quality filtering of the raw reads, samples with read loss >90% were excluded from further analysis to avoid biases associated with low microbial biomass and host-dominated sequencing profiles. The number of raw and filtered reads remaining for all samples are reported in Supplementary Table 1.

2.2.2. Taxonomic profiling, metagenome assembly, and MAG reconstruction

Taxonomic profiling was performed on the clean filtered reads using Kraken2 v2.0.8-beta (Wood et al., 2019) with default settings and a modified version of the PlusPF database (Langmead, 2024) updated on January 12, 2024, and modified by adding the *Bos taurus* reference genome (GCA_002263795.4). Bracken v2.5 (Lu et al., 2017) with parameters "-r 150, -l S", was applied to refine taxonomic assignments and estimate species-level abundances, using the same indexes built from the Kraken2 database. Among those taxa detected in at least 90% of the samples from a niche (e.g., summer slaughter hall), niche-specific core microbiome was defined as composed of species showing a relative abundance ≥1% in ≥20% of the samples from that niche, as previously suggested by Barcenilla, Cobo-Díaz, Puente, et al. (2024), to ensure robustness against low-abundance noise.

Filtered reads from each sample were assembled into contigs using MEGAHIT v1.2.2 (Li et al., 2015) with the parameter "–k-list 21,33,55,71,81,91", and contigs smaller than 1000 bp were discarded for further analysis. Filtered reads were mapped to their respective sample's contigs using Bowtie2 v2.2.9 (Langmead & Salzberg, 2012) with "–very-sensitive-local" and "–no-unal" options. The *jgi_summarize_bam_contig_depths.pl* script, from MetaBAT v2.12.1 (Kang et al., 2019), was used to calculate contig depth values from the *.sam* files obtained by bowtie2 alignment. Contigs and the files resulting from the previous step mapping were processed with MetaBAT2 v2.12.1 (Kang et al., 2019) with "-m 1500 –unbinned" parameters to group contigs into bins, and the quality of bins was assessed using CheckM2 v1.0.1 (Chklovski et al., 2023). Metagenome-Assembled Genomes (MAGs) showing completeness ≥50% and contamination ≤10% ("medium/high quality" MAGs, according to Benoit et al. (2024)) were retained for further analysis.

Species-level genome bins (SGBs) were defined by clustering MAGs at ≥95% of Average Nucleotide Identity (ANI) threshold. Genomic distances were initially estimated using MASH v1.1 (Ondov et al., 2016), followed by high-resolution pairwise ANI calculations using FastANI v1.33 (Jain et al., 2018).

To reduce spurious matches arising from limited genomic overlap, an alignment fraction filter was applied, calculated from FastANI output as the proportion of mapped genome fragments (n_mappings / n_fragments). Genome pairs were retained for clustering if they satisfied ANI ≥95% and alignment fraction ≥0.2, a threshold selected to retain partially reconstructed MAGs while minimizing spurious matches (Supplementary Fig. 1).

Genome clustering was performed by constructing a similarity graph from retained genome pairs and identifying connected components. This graph-based approach is widely used for defining SGBs based on ANI thresholds (Almeida et al., 2021; Pasolli et al., 2019). Taxonomic assignment of MAGs was conducted using the Genome Taxonomy Database Toolkit (GTDB-Tk) v2.4.0 (Chaumeil et al., 2020) using "classify_wf" pipeline and the database release 220.

2.2.3. Functional annotation of the assembled contigs

Coding sequences (CDSs) were predicted on contigs through MetaGeneMark heuristic model v1 (Zhu et al., 2010) using "-a -d -f G" parameters. The functional potential of the assembled contigs was characterized using homology searches against several curated databases, and a hit was considered valid if the alignment covered ≥90% of the reference gene length and ≥ 90% sequence identity, to ensure high-confidence functional assignments and minimize false positives. Antimicrobial resistance (AMR) and biocide-resistance genes were identified by searching the predicted CDSs against the Comprehensive Antibiotic Resistance Database (CARD v3.2.4) (Alcock et al., 2023) and the BacMet2 database (Pal et al., 2014), respectively, using BLASTx (Camacho et al., 2009). Virulence factor genes were detected using BLASTn (Camacho et al., 2009) searches against the core nucleotide dataset of the Virulence Factor Database (2022 release) (Liu et al., 2022). Finally, to identify spoilage-related genes, an extensive literature search was conducted to construct a custom protein database focusing on meat spoilage. This database comprises 336 curated spoilage-related genes involved in key pathways, including protein metabolism, lipid metabolism, sulfur metabolism, regulatory pathways, siderophore production, biofilm formation, stress adaptation, and quorum sensing, all of which were verified using the UniProt database to confirm their functions against experimentally validated reference proteins. This core set of genes was expanded with 4653 orthologous sequences sourced from a diverse range of bacterial species in the NCBI protein database. The custom spoilage gene database, along with annotations, is publicly available online (DOI: https://doi.org/10.5281/zenodo.17494165). Additionally, bacteriocin-related genes, including structural peptides and associated functional machinery were identified within lactic acid bacteria (LAB) MAGs using sequence similarity searches against the UniProtKB/Swiss-Prot database (accessed February 2026; The UniProt Consortium, 2025). Candidate hits were initially retrieved using a comprehensive set of bacteriocin-associated keywords and functional

domains to capture both well-characterized and divergent homologs. To ensure sensitivity toward divergent and potentially novel bacteriocin systems, which are typically short and frequently fragmented during metagenomic assembly, relatively permissive thresholds of ≥30% amino acid identity and ≥ 30% query coverage were applied. Applying stricter coverage filters resulted in the loss of nearly all bacteriocin detections due to the partial reconstruction of these small genetic elements. Functional annotation and classification of hits into core peptides, transport systems, modification enzymes, and immunity proteins were subsequently refined based on UniProt protein descriptions and gene annotations (Supplementary Table 2).

To achieve a genome-resolved functional landscape, downstream analyses were restricted to contigs successfully binned into medium- and high-quality MAGs. Functional gene abundances were calculated as Reads Per Kilobase of gene per Million reads (RPKM) to normalize for differences in gene length and sequencing depth. At the community level, RPKM values were summed across all target genes within each functional group per sample to estimate the total functional load. At the species level, RPKM values were summed for genes assigned to each genome or species to estimate the functional contribution of individual taxa. This approach enabled comparison of functional potential at both the community and genome/species levels.

The assembled contigs from each sample were also analyzed to identify bacteriophages using the end-to-end workflow of PhaBOX2 v2.1.11 (Shang et al., 2023) against the phabox_db_v2 internal database. This resulted in predictions for the viral taxonomy and lifestyles (lytic or temperate), along with prediction scores and confidence values, and predicted potential bacterial hosts (Shang et al., 2023). The assigned viral contigs from PhaBOX2 were quantified to obtain abundance values using Bowtie2 v2.2.9, using –very-sensitive-local and –no-unal parameters by mapping the raw reads from each sample back to their predicted phage contigs.

2.3. Statistical analysis and visualization

All statistical analyses were conducted using R v4.3.3 (R Core Team, 2024). The map shown in Fig. 1 was generated using the *rnaturalearth* v1.2.0 (Massicotte & South, 2026) and *rnaturalearthdata* v1.0.0 (South et al., 2024) R-packages. Simpson diversity was calculated using the 'diversity' function, and observed richness was calculated using the 'specnumber' function from the *vegan* R-package v2.7.3 (Oksanen et al., 2026). To reduce the influence of spurious low-abundance assignments, a 0.01% relative abundance threshold was applied prior to calculating Richness. The results were visualized as boxplots using the *ggplot2* R-package v4.0.3 (Wickham, 2016), with individual data points superimposed using the *ggbeeswarm* R-package v0.7.3 (Clarke et al., 2025). Significance values were added to these plots using the 'compare_means' function in the *ggpubr* R-package v0.6.3 (Kassambara, 2026), through the Kruskal-Wallis and Pairwise Wilcoxon rank-sum tests. Statistical significance was set at $p < 0.05$, and all *p*-values were adjusted for multiple comparisons through the Benjamini and Hochberg method. For the taxonomic level stacked bar charts and heatmaps, the *ggplot2* and *pheatmap* v1.0.13 (Kolde, 2025) R-packages were used, while the phylogenomic tree was developed using the *ggtree* R-package v4.3.0 (Yu et al., 2017).

Beta diversity was assessed by computing a pairwise dissimilarity distance matrix based on the Bray-Curtis distance using the function 'vegdist' from the *vegan* R-package. A principal coordinate analysis (PCoA) was then performed on this matrix using the 'cmdscale' function from the *base* R-package. Similarly, the effects of the metadata variables (i.e., seasons, locations, and surfaces) on the overall community composition were tested using a permutational multivariate analysis of variance (PERMANOVA) with the 'adonis2' function (999 permutations). Furthermore, intra-group dispersion homogeneity was assessed using the 'betadisper' function from the *vegan* R-package to verify homogeneity of group dispersions.

Additionally, to evaluate statistical associations between bacteriophage abundance and predicted bacterial host abundance, linear mixed-effects models were implemented using the *lme4* v2.0.1 (Bates et al., 2015) and *lmerTest* v3.2.1 (Kuznetsova et al., 2017) R-packages. Bacterial host abundance was used as the response variable, while phage abundance and scaled sample load, defined as sequencing depth normalized and scaled across samples, were included as fixed effects. Processing location and predicted bacterial host were included as random effects. Season was included in candidate models but was not retained in the final selected model. Approximately 35 candidate models were evaluated, and the final model was selected based on model parsimony and the lowest Akaike Information Criterion (AIC) and Bayesian Information Criterion (BIC). The selected model structure was as follows:

$$lmer\Big(log\_Host\_Abundance \sim log\_Phage\_Abundance^{*}\ Scaled\_Load + (1 \mid major\_location) + (1 \mid Host)\Big)$$

The same modeling framework was then applied at the location and individual sample-point levels. Sample-point level model results for key meat-relevant species that showed statistically significant negative associations with their predicted bacteriophages were visualized using forest plots from the *ggforestplotR* v0.2.2 (Richardson, 2026) R-package, with positive predictive trends not shown to improve visualization clarity.

2.4. Data availability

The raw shotgun metagenomic sequencing data generated in this study are publicly available in the NCBI Sequence Read Archive (SRA) under BioProject accession number PRJNA1233666. Detailed metadata for all recovered MAGs including SRA accession, BioSample accessions, ANI similarity to reference genomes, and SGB identifiers are provided alongside the FASTA files at Doi: https://doi.org/10.5281/zenodo.18904513 (Supplementary Table 5).

3. Results

3.1. Microbial diversity decreases along the meat processing chain

Principal Coordinate Analysis (PCoA) based on Bray–Curtis dissimilarities of samples collected during active production showed a significant effect of the interaction between season and surface type on microbial community composition (PERMANOVA, $R^2 = 0.041$, $p < 0.001$; Fig. 2A). One cluster mainly included processing environmental surfaces, including food-contact and non-food-contact surfaces, together with carcasses, whereas a separate cluster included meat and retail meat products (Fig. 2A and Supplementary Fig. 2A). Interestingly, microbial richness decreased progressively along the processing chain across facilities and seasons (Fig. 2B). The highest mean species richness was observed in the farming environment (Farm in summer: 2271 ± 495; Farm in winter: 1106 ± 400; Lairage hall in summer: 1282 ± 311;

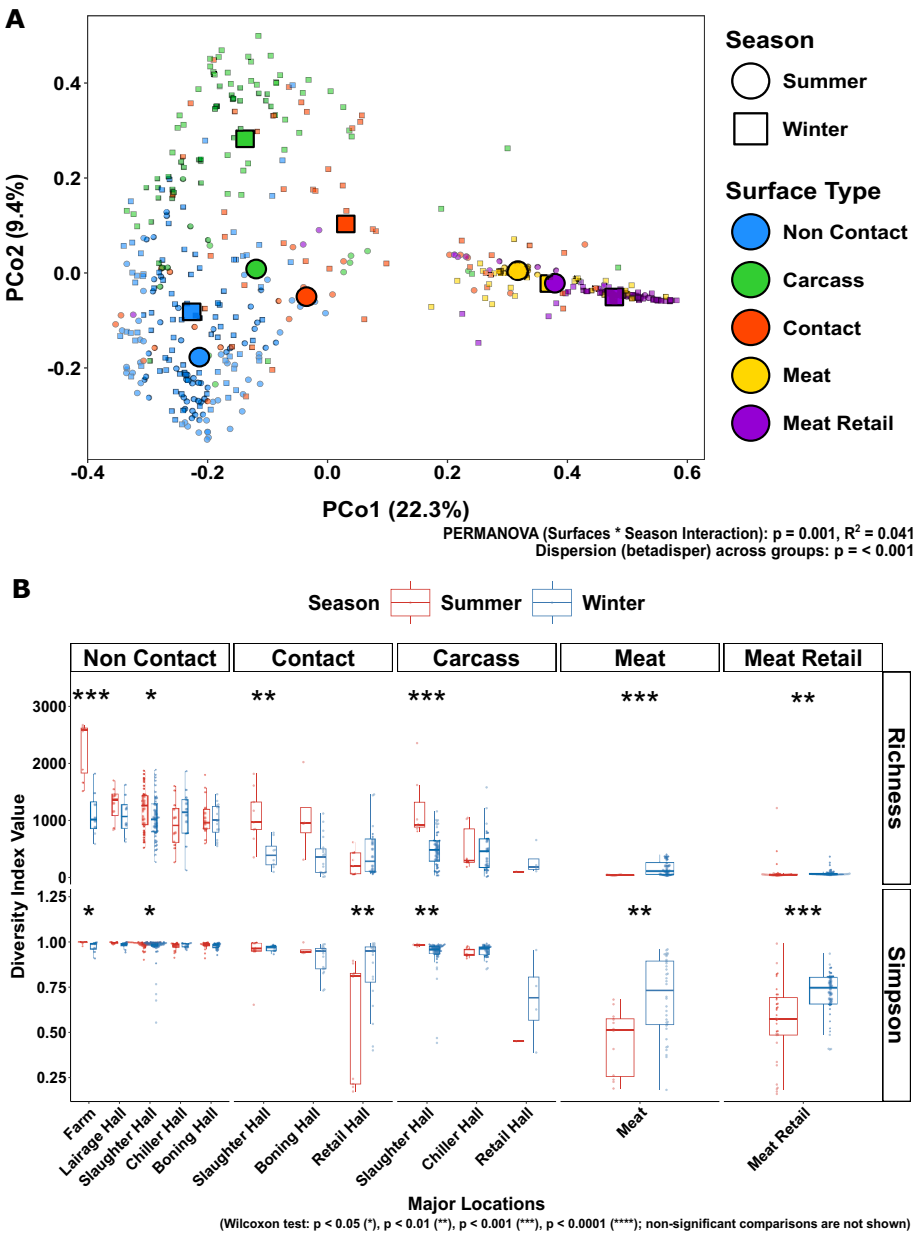

Fig. 2. Microbial alpha and beta diversity across sampling locations and seasons. The diversity indices were calculated for processing surfaces and final meat products, excluding post-cleaning samples to isolate baseline facility and product microbiota. (A) Principal Coordinate Analysis (PCoA) based on Bray-Curtis dissimilarity illustrating community divergence across production niches. Point colors denote specific surface types or meat products, while shapes indicate seasonality. (B) Comparative alpha diversity analysis across processing locations and final products, grouped by season. Statistical significance between seasonal groups was determined using the Wilcoxon rank-sum test: $p < 0.05$ (*), $p < 0.01$ (**), $p < 0.001$ (***), $p < 0.0001$ (****).

Lairage hall in winter: 1083 ± 355). Richness then decreased toward the final stages, with lower values recorded in the retail hall (summer: 361 ± 253; winter: 464 ± 386), meat products (summer: 41 ± 8; winter: 160 ± 125), and retail meat samples (summer: 102 ± 215; winter: 79 ± 61). Notably, summer showed higher richness within the processing environment, whereas winter showed higher richness in meat products (Supplementary Fig. 2B). This progressive reduction was consistent across both food-contact and non-food-contact surfaces, regardless of season (Supplementary Fig. 2C–E). No significant differences in species richness were observed between seasons, except at the farm ($p < 0.001$), slaughter hall ($p < 0.01$), meat product stage ($p < 0.001$), and retail meat stage ($p < 0.01$) (Fig. 2B). A similar trend of declining richness was observed between early and late meat maturation stages, although differences were not significant at individual maturation time points (Supplementary Fig. 2F). Although environmental species richness decreased along the process, the Simpson diversity index remained relatively high and stable, indicating that community dominance patterns changed less strongly than richness (Fig. 2B). The main exception was observed in contact surfaces and carcasses from the retail hall, where lower Simpson diversity suggested a more uneven community structure (Fig. 2B). Furthermore, microbial diversity in meat decreased during both long-term maturation and the retail storage phase (Supplementary Fig. 2E–G). Interestingly, a significant temporal shift in the Simpson diversity index between early and late maturation stages was detected only in winter, but not in summer (Supplementary Fig. 2G). The core microbial community profile showed limited variation following sanitation, with no significant differences detected between active-production and post-cleaning samples across processing stages (Wilcoxon rank-sum test, FDR-adjusted $p > 0.05$; Supplementary Fig. 2H).

3.2. Final meat products show a lower microbial diversity than the processing environment

The meat processing environment showed a seasonally dynamic taxonomic composition, with a clear progression from a diverse microbial community in farm samples to a more specialized, LAB-dominated community in the final processing stages. The winter core community was dominated by *Bifidobacterium pseudolongum* and *Cutibacterium acnes* in many locations compared to the more diverse array of microbial species characterizing the core microbiome in summer, including *Acinetobacter johnsonii* and *Corynebacterium xerosis* (Supplementary Fig. 3A–D). Beyond these seasonal core patterns, microbial community composition differed significantly among the processing locations, regardless of the season (Supplementary Table 3). Furthermore, we narrowed down our focus on 49 key indicator species (30 known spoilage species and 19 species potentially linked to food safety concerns) relevant to the facility hygiene and safety profiles (the full list is provided in Supplementary Table 4). Notably, these targeted species were largely undetected or present at very low relative abundances in upstream processing environments, including farm, lairage, and non-food contact surfaces such as drains, floors, and walls (Supplementary Fig. 4). These environments were instead characterized by the persistent presence of background environmental taxa, such as *Acinetobacter johnsonii*, which were consistently detected across locations and seasons despite maintaining a low relative abundance. Furthermore, by tracking these selected taxa, we observed that spoilage-associated species dominated the meat products, whereas species linked to food safety concerns were detected at very low relative abundances in meat products, despite the higher microbial richness observed in processing environment. The spoilage-associated community showed a substantial increase throughout the production chain, increasing from 2.59 ± 4.10% on non-contact surfaces to high relative abundance in meat (83.2 ± 20.8%) and retail meat products (90.7 ± 19.2%). This pattern was largely driven by the increased relative abundance of cold-tolerant taxa, including *C. divergens* (average value of 28.7% in meat) and *P. carnosus* (22.5% in meat retail) (Fig. 3A–B).

The processing environment also harboured several species potentially linked to food safety concerns, with the total relative abundance peaking on the contact surfaces (2.02 ± 3.96%) and carcasses (1.72 ± 2.69%), primarily led by *Enterococcus faecium* (0.56%) and *Clostridium perfringens* (0.35%). Although their abundance decreased in final meat products (0.32 ± 0.18%), specific taxa were detected at higher relative abundances in localized retail meat environments (total pathogen abundance: 1.26 ± 7.19%; most abundant: *Klebsiella pneumoniae* 0.79% and *Yersinia enterocolitica* at 0.33%) (Fig. 3C–D).

Interestingly, the operators' hands and knives emerged as potential transfer points for meat-associated spoilage bacteria, particularly in the Boning and Retail Halls, as we observed high relative abundances of *P. carnosus* (34.1%) and *Dellaglioa algida* (16.2%) on operators' hands sampled in winter. Consistently, *D. algida* dominated on knives (15.2%),

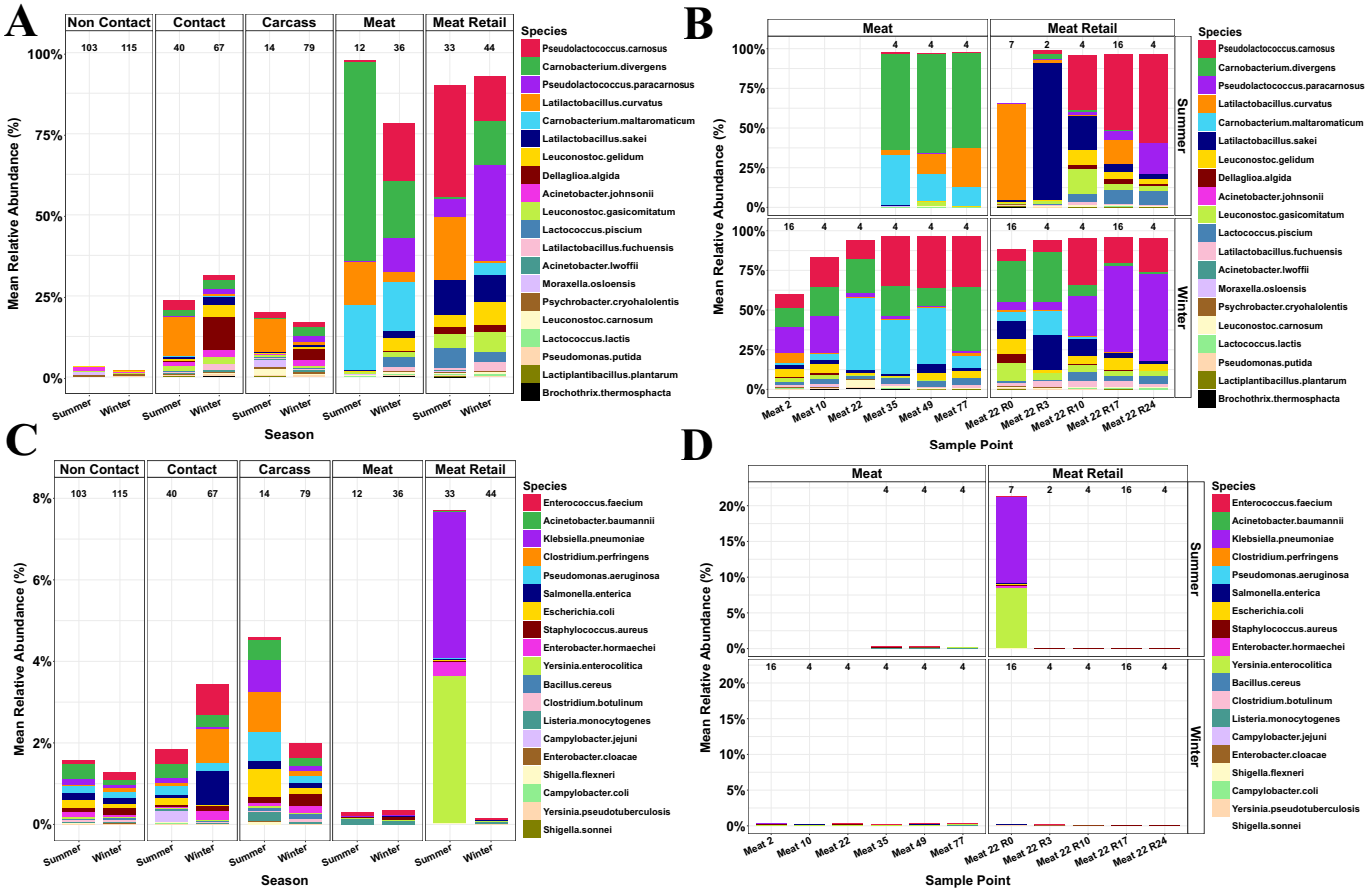

Fig. 3. Distribution of spoilage and pathogenic taxa across surfaces, maturation stages and seasons. Taxonomic profiles represent the full longitudinal dataset, including baseline production and post-sanitation monitoring. (A) Mean relative abundance (% of bacterial reads) of spoilage-associated species across processing surfaces and final meat products. Taxa are ranked by decreasing cumulative abundance across the full dataset; for clarity, only the top 20 spoilage-associated species (out of 30) are shown in panels A and B, while all 19 species potentially linked to food safety concerns are displayed in panels C and D. Integers above stacked bars indicate the sample size (n) for each experimental group. (B) Mean relative abundance (% of bacterial reads) of spoilage species in matured meat products at each specific maturation timepoint. (C) Mean relative abundance (% of bacterial reads) of pathogenic species on processing surfaces and in final meat products. (D) Mean relative abundance (% of bacterial reads) of pathogenic species in matured meat products at each specific maturation timepoint.

and primals at debagging (20.2%) in the Retail Hall (Supplementary Fig. 4A). Conversely, these same sample points in summer were dominated by *Latilactobacillus curvatus* on operators' hands (44.3%), knives (28.2%), and primals (73.9%) (Supplementary Fig. 4A). Species potentially associated with food safety concerns were also detected. Among these, sequences assigned to *Salmonella enterica* showed their highest relative abundance in operators' hands and knife samples, reaching approximately 9.1% in the aggregated dataset (Supplementary Fig. 4C). Furthermore, vacuum bags were found to contain species potentially linked to food safety concerns, including *E. faecium*, *Acinetobacter baumannii*, *Staphylococcus aureus*, *Pseudomonas aeruginosa*, and *Enterobacter hormaechei,* with a total mean relative abundance of 13% in winter and 2.2% in summer (Supplementary Fig. 4C).

3.3. Sanitation reshapes the taxonomic composition of the environmental microbiome

Sanitation reduced the relative abundance of dominant spoilage-associated organisms in Retail Hall, such as *L. curvatus*, which decreased from 54.0% to 4.12%, and *C. divergens,* dropping from 14.0% to below detection levels in summer. Similarly, *D. algida,* the dominant winter species, declined from 23.2% to 3.85% (Supplementary Fig. 4B). However, the abundance of some species was minimally affected by sanitation. Notably, *A. johnsonii* persisted across all locations and seasons after sanitation. Conversely, the potential pathogenic taxa showed variable response to sanitation depending on season and processing location. In particular, *E. faecium*, *A. baumannii*, *K. pneumoniae*, *P. aeruginosa*, *S. enterica*, *S. aureus, and Escherichia coli* were consistently detected after sanitation across locations and seasons. These observations indicate that, while sanitation reduced the abundance of several dominant spoilage-associated species, certain species potentially linked to food safety concerns remained detectable across locations and seasons after sanitation (Supplementary Fig. 4D).

3.4. Surface types and maturation protocols are associated with the enrichment of meat-specialized LAB

A consistent trend of microbial succession from a diverse environmental community to a specialized, LAB-dominated profile in meat samples was observed in both seasons. In particular, contact surfaces and carcasses showed consistently higher relative abundances of LAB consortia (*Latilactobacillus, Carnobacterium, Pseudolactococcus, Dellaglioa*) across seasons. This was seasonally dependent: summer contact and carcass surfaces were dominated by L. *curvatus*, whereas *D. algida* dominated in winter (Fig. 3A). Conversely, the microbial community on meat products remained relatively stable across seasons, consistent with the controlled conditions during maturation. However, maturation was associated with changes in microbiome composition. In detail, during long-term continuous maturation in summer, *C. divergens* was consistently the most abundant species (average relative abundance between 61 and 63%), while *C. maltaromaticum* was steadily displaced by L. *curvatus* over time (Fig. 3B). In winter, a diverse initial community was shifted toward co-dominance by *P. carnosus* (31.8% on average) and *C. divergens* (40.6%), while *P. paracarnosus* decreased sharply (23.2% in meat matured for 2 days, 0.5% after 77 days) (Fig. 3B). Moreover, during meat retail maturation in summer, an initial dominance of L. *curvatus* (60.2%) was shifted toward dominance by L. *sakei* (86%) by day 3, which was then followed by increased relative abundance of *P. carnosus* (55.6%) and *P. paracarnosus* (19.1%) by the end of the retail shelf life. In winter, the early stages (day 0–3) were co-dominated by *Latilactobacillus*, *Pseudolactococcus*, and *Carnobacterium*, transitioning to a dominance by *P. paracarnosus* (54.6%) and *P. carnosus* (21.3%) at day 24 (Fig. 3B).

Finally, a low-level but persistent occurrence of species potentially linked to food safety concerns was observed across environmental surfaces and seasons. These species, including *E. faecium*, *A. baumannii*, *K. pneumoniae*, *C. perfringens*, *S. aureus*, *S. enterica*, *E. coli,* and *Listeria monocytogenes* were consistently present across all surface types in both seasons, generally maintaining a relative abundance below 2% (Fig. 3C). Moreover, throughout both maturation processes, their relative abundances decreased further (<0.2%) across all time points (Fig. 3D).

3.5. The production environment shows a broad functional gene repertoire

We then estimated the prevalence and abundance of genes associated with food spoilage, food safety risks, and microbial stress adaptation against biotic/abiotic stresses. The overall abundance (RPKM) of spoilage-related genes was higher in summer than in winter, and summer carcasses showed the highest RPKM value (Wilcoxon rank sum test, p-value <0.001; Fig. 4A). This functional load was particularly elevated in the summer Retail Hall, followed by the summer Chiller Hall (Supplementary Fig. 5A). Among spoilage-associated genes, those involved in biofilm formation were the most abundant across environmental surfaces, particularly in Chiller, Boning, and Retail Halls during summer (Supplementary Fig. 5B) and were predominantly associated with *P. paracarnosus* and *D. algida* (Supplementary Fig. 5C). Importantly, biofilm-associated genes showed a higher mean functional load in post-cleaning samples than in during-production samples (820 vs. 257 RPKM; 3.19-fold increase), with only a modest increase in median load (282 vs. 182 RPKM; Supplementary Fig. 5D), although this difference was not statistically significant and showed high variability among post-cleaning samples (Wilcoxon rank-sum test, $p = 0.38$). Nevertheless, biofilm-associated genes remained detectable across processing environments irrespective of sanitation status. At the same time, retail meat samples showed a high abundance of quorum-sensing genes linked to *P. carnosus*, suggesting the potential for coordinated microbial activity associated with spoilage on the final product across seasons (Fig. 4B; Supplementary Fig. 5C–F).

In addition, genes conferring resistance to antimicrobial compounds were generally detected at low abundances and were not strongly influenced by season, except for carcasses from the summer sampling, where antimicrobial resistance was higher compared to the samples collected in winter (Fig. 4C). Overall, macrolide resistance genes were mainly detected on winter contact surfaces, while tetracycline resistance genes were more abundant in retail meat samples and were associated with dominant spoilage taxa such as *P. paracarnosus* and *C. maltaromaticum* (Fig. 4D; Supplementary Fig. 6). Virulence and biocide resistance genes were detected at low abundances across processing environments and were nearly absent in meat products (Supplementary Figs. 7 and 8). While LAB species dominated spoilage-associated communities, they showed minimal representation of virulence-associated genes. In parallel, virulence-encoding species were widely distributed across processing surfaces. Particularly, *E. faecalis* was consistently detected throughout the production chain across both seasons and was associated with multiple functional traits, including spoilage, antimicrobial resistance, biocide resistance, and virulence (Fig. 4E).

Moreover, the observed microbial succession during meat maturation was associated with changes in bacteriocin-associated functional potential among LAB. During long-term maturation, *Carnobacterium* species increased in relative abundance together with a diverse repertoire of bacteriocin-associated genes, including a high relative abundance of Class IIb (sibling) systems, such as Lactococcin G (16.4 RPKM in *C. maltaromaticum*), as well as core bacteriocin peptides including antilisterial subtilosins encoded by *AlbA* and *AlbE* (9.6 RPKM in *C. divergens*) (Supplementary Figs. 9A–B).

However, during the retail phase, a shift in both taxonomic composition and functional profiles was observed, with *Pseudolactococcus* species becoming more prominent in retail meat products. This transition was associated with distinct bacteriocin-related functional patterns. Specifically, *P. paracarnosus* showed a higher relative contribution of

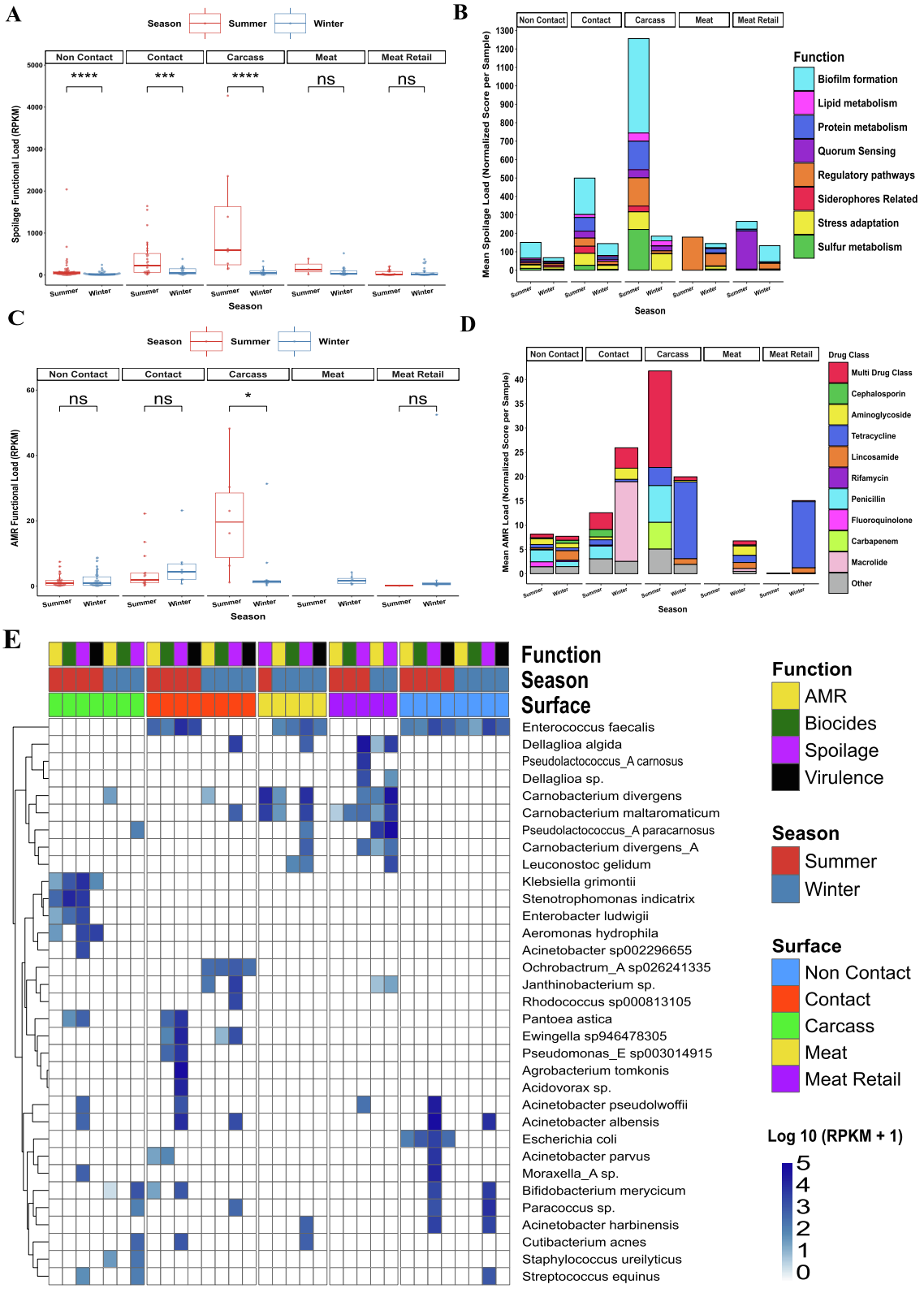

Fig. 4. Abundance and composition of functional genes in recovered genomes on processing surfaces and in final meat products across seasons. Functional gene loads (RPKM) and composition for spoilage genes (A, B) and antimicrobial resistance genes (C, D). Gene loads were compared between groups using the Wilcoxon rank-sum test. Asterisks indicate significance: $p < 0.05$ (*), $p < 0.01$ (**), $p < 0.001$ (***), $p < 0.0001$ (****). "ns" indicates not significant values. (E) Heatmap of the top reservoir species carrying high functional gene loads across processing surfaces and final meat products. Functional gene abundances (RPKM) are presented on a log10(RPKM +1) scale. The heatmap is filtered to display only the top 2 species from each niche (e.g., Carcass in Summer) that carry high functional loads and are shared across at least two niches.

post-translational modification enzymes (52.4% of bacteriocin-related gene load), including L-threonine dehydratase (97.4 RPKM) required for peptide maturation. In parallel, *P. carnosus* was associated with increased allocation of functional potential in protection and export, allocating 26.5% of its functional potential to immunity proteins (132.3 RPKM) and transport systems associated with Class IIb bacteriocin systems such as lactobin A and Lactococcin 972 (Supplementary Figs. 9A–B).

3.6. Bacteriophages are associated with microbiome structuring along the production chain

Bacteriophage communities showed higher diversity at initial processing locations and on non-contact surfaces, with lower diversity observed on contact surfaces and carcasses in later processing stages (Supplementary Fig. 10A–B). Taxonomic profiling revealed that the community was dominated by phages predicted to target *E. coli* across seasons. Similarly, phages predicted to target *A. baumannii* were more prevalent and abundant across processing locations and surfaces in summer. In addition, a consistent set of phages predicted to target *Bacillus subtilis, S. enterica, K. pneumoniae,* and *P. aeruginosa* was detected across processing locations and surfaces. Conversely, phages predicted to target spoilage-associated species such as *Brochothrix thermosphacta, C. divergens,* and *L. lactis* were more prevalent and abundant in matured meat products across seasons (Fig. 5A; Supplementary Fig. 10C). Moreover, a linear mixed-effects model evaluating the correlative association between phage abundance and predicted bacterial host abundance revealed a strong positive association across all samples ($\beta = 0.48$, $p < 0.001$; Fig. 5B). However, significant negative correlations (FDR < 0.05) were observed between phage abundance and the abundance of some predicted pathogen hosts within specific processing niches (Fig. 5C; Supplementary Fig. 10D), suggesting potential phage–host interactions, although direct predation cannot be inferred from these data. For instance, low relative abundance of L. *monocytogenes* coincided with higher abundance of its predicted phages on non-contact surfaces in the Slaughter Hall ($\beta = -0.40$; Fig. 5C; Supplementary Fig. 10D). However, the strongest negative associations between phages and their predicted hosts were observed in matured meat, where L. *monocytogenes* showed lower abundance at day 10 ($\beta = -0.73$), and *S. aureus* showed lower abundance at day 77 ($\beta = -0.39$) (Fig. 5D). Similarly, in retail meat samples, significant negative correlations were detected for *A. baumannii* ($\beta = -1.12$) and *P. aeruginosa* ($\beta = -0.97$) at day 17, as well as *S. enterica* ($\beta = -0.62$) at day 24 (Fig. 5D).

3.7. Genome-resolved analysis reveals prevalent uncharacterized lineages in the meat production chain

A total of 4475 medium/high-quality MAGs were recovered, of which 4283 were assigned to 1173 species-level genome bins (SGBs), while 192 MAGs remained unassigned after FastANI-based clustering

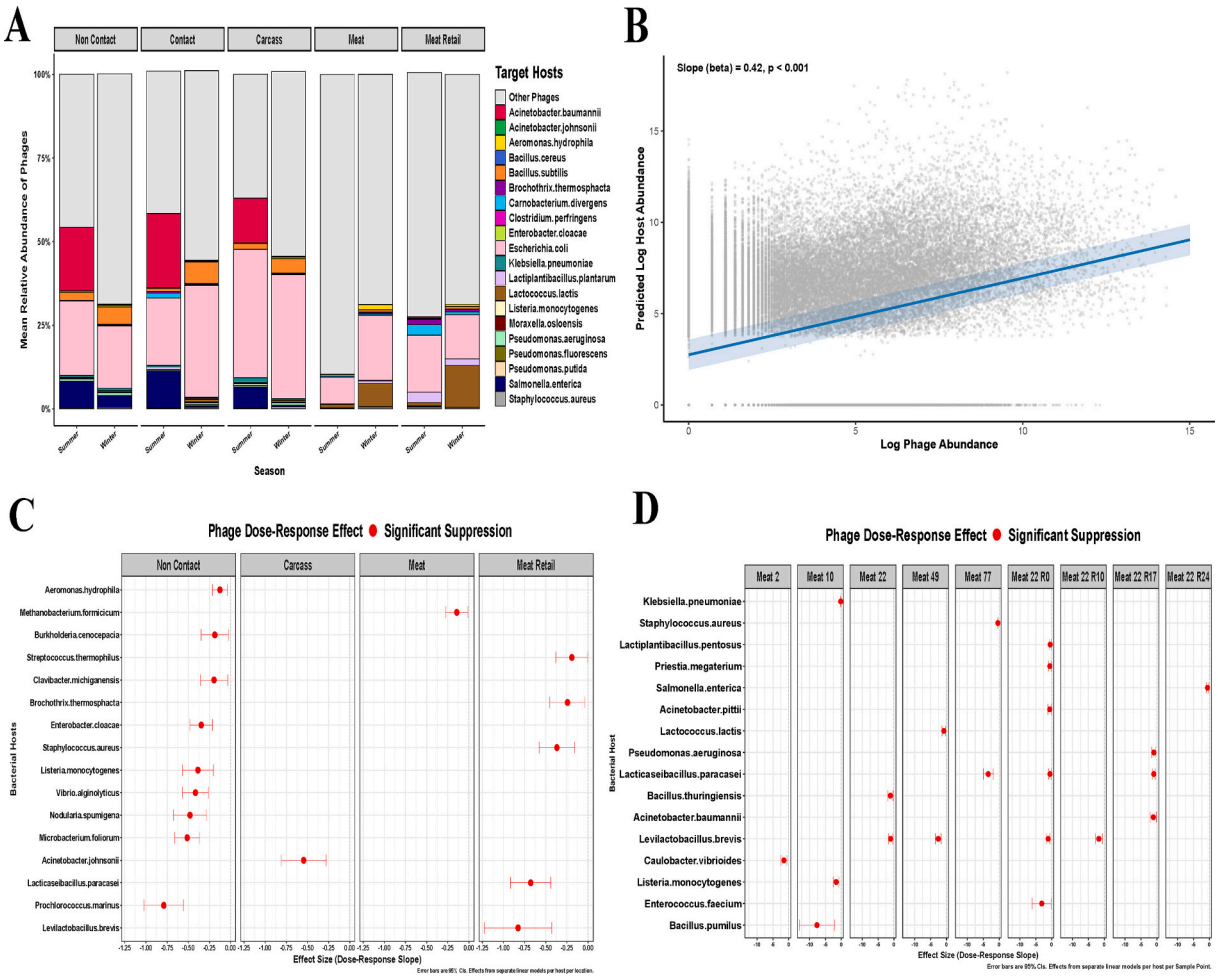

Fig. 5. Abundance, composition, and associations of bacteriophages with their predicted bacterial hosts across processing surfaces and final meat products across seasons. (A) Mean relative abundance (%) and composition of bacteriophages (predicted host names are shown in the legend) on processing surfaces and in meat products. (B) Linear mixed-effects model showing the association between phage abundance and predicted host abundance across the whole dataset. (C) Associations between phages and their predicted hosts on processing surfaces and final meat products. (D) Associations between phage abundance and predicted host abundance at each meat maturation time point.

and alignment-fraction filtering (Supplementary Table 5). Genome-resolved analysis confirmed a clear ecological divergence between processing environments and meat products. Because MAG counts reflect genome recovery rather than community relative abundance, these patterns were interpreted as genome-resolved representation of dominant or recurrent taxa rather than direct abundance estimates. The environmental microbiome composition shifted seasonally: the summer environment was dominated by *Parageobacillus thermoglucosidasius_A* (n = 28 MAGs), whereas winter environments were dominated by *Bifidobacterium globosum* (n = 58 MAGs) and *Jeotgalicoccus sp003513765* (n = 49 MAGs). *Corynebacterium xerosis* (summer: n = 21; winter: n = 34 MAGs) remained a consistent resident across seasons. In contrast, meat products were dominated by spoilage-associated taxa. *P. carnosus* (n = 23 MAGs) and *D. algida* (n = 18 MAGs) dominated the meat microbiome in summer, whereas winter meat was dominated by *Latilactobacillus fuchuensis* (n = 39 MAGs) and *C. divergens* (n = 32 MAGs).

Interestingly, nearly 40% of the total MAGs (1773 out of 4475 MAGs) were identified as putative novel species not assigned to any currently represented species in the GTDB database, including 486 near-complete MAGs, defined as completeness ≥90% and contamination <5%. Within this group, a specific subset of 126 MAGs could not be assigned to any known genera and were mainly affiliated with the phyla Bacillota_A (n = 54), Actinomycetota (n = 47), and Pseudomonadota (n = 8). Among the remaining novel MAGs that could be assigned at the genus level, *Corynebacterium* (n = 121) and *Paracoccus* (n = 55) were the most prevalent (Fig. 6).

Only 18 out of the 29 targeted spoilage or pathogenic genera were recovered at the MAG level (Supplementary Table 3). *Listeria, Salmonella, Campylobacter, Shigella,* and *Yersinia,* alongside spoilage genera such as *Pseudomonas, Serratia,* and *Weissella,* were not recovered as MAGs, likely reflecting their low abundance, limited genome coverage, or poor binning recovery rather than complete absence from the dataset. In contrast, MAGs assigned to resilient spoilage-associated taxa were recovered, including *Latilactobacillus* (n = 151 MAGs; 3.37% of obtained MAGs), *Psychrobacter* (n = 107; 2.39%), *Leuconostoc* (n = 101; 2.26%), and *Carnobacterium* (n = 92; 2.06%). Some tracked species potentially linked to food safety concerns, such as *Clostridium* (n = 3; 0.07%), *Escherichia* (n = 1; 0.02%), *Klebsiella* (n = 3; 0.07%), and *Staphylococcus* (n = 8; 0.18%), represented a very small fraction of the total reconstructed MAGs and were mainly recovered from environmental surfaces (Fig. 6).

Beyond individual genomes, FastANI-based clustering assigned 4283 MAGs into 1173 distinct SGBs, revealing a highly partitioned genome-resolved microbiome. Among these, 648 SGBs were singletons, each represented by a single MAG. These singleton SGBs therefore correspond to genomes that passed the clustering workflow but did not group with any other MAG at the defined ANI ≥95% and alignment fraction ≥0.2 thresholds. In addition, 192 MAGs were not assigned to any SGB because they did not generate valid pairwise FastANI links after alignment-fraction filtering. These MAGs were retained as unclustered genomes rather than being forced into singleton SGBs. Together, singleton SGBs and unclustered MAGs represented 840 MAGs, highlighting a substantial fraction of rare, weakly connected, or phylogenetically isolated lineages within the dataset. In contrast, 222 multi-MAG SGBs accounted for 62.5% of all reconstructed MAGs, indicating that a limited number of genomic clusters dominated the dataset across samples and seasons. Meat products showed a strong filtering effect, narrowing genome-resolved richness to 70 unique SGBs (Supplementary Fig. 11).

The 840 singleton-associated and unclustered MAGs represented a secondary functional reservoir. These rare or unclustered lineages represented 8.2% (60,461 RPKM) of the total functional load. Specifically, 7.2% was linked to spoilage-related potential, 0.2% to AMR markers, predominantly *tet(S)* and *mphO* genes, 0.6% to biocide resistance, and 0.2% to virulence-associated potential. In contrast, SGBs assigned to known taxa accounted for 84.2% (9154 RPKM) of the total virulence-related RPKM (10,876). This load was primarily associated with opportunistic residents such as *Stenotrophomonas* and *Enterococcus,* characterized by multidrug efflux and secretion systems. The total spoilage load reached 685,961 RPKM, with known SGBs accounting for 92.3% of this burden (1153 RPKM per MAG on average). This dominance was mainly associated with a resilient LAB core in meat products, specifically *P. paracarnosus* (sum = 71,529 RPKM) and *C. divergens* (sum = 60,711 RPKM).

4. Discussion

Meat processing environments can be considered as dynamic reservoirs of complex microbiomes that may provide a primary source of microbial contamination for meat products (Barcenilla, Cobo-Díaz, Puente, et al., 2024; Fagerlund et al., 2021; Zwirzitz et al., 2020). In the present study, we observed higher microbial diversity on processing surfaces than in meat samples, as previously reported (Barcenilla, Cobo-Díaz, Puente, et al., 2024; Palanisamy et al., 2023; Sequino et al., 2024). In particular, the highest species richness was observed on surfaces during active production in the Slaughter Hall. Indeed, slaughtering is widely recognized as a major point at risk of cross-contamination due to the possible spread of microbes from animal skin, legs, and intestinal content during evisceration (Nørrung et al., 2009; Wheatley et al., 2014). However, our targeted-species analysis showed that key spoilage- and food safety-associated taxa were largely undetected or present at very low relative abundances in upstream pre-maturation environments, including farm, lairage, slaughter, and non-food-contact surfaces. These environments were instead characterized by persistent background taxa, such as *A. johnsonii,* which were widespread but generally low in abundance. This suggests that high environmental richness does not necessarily translate into direct contamination pressure from the upstream reservoirs. Nevertheless, downstream food-contact surfaces and handling-associated points appeared to contribute more strongly to the transfer of meat-relevant taxa.

In contrast, environmental samples from the Chiller Hall, where carcasses were stored at 0–3 °C for 36 h, showed lower richness, probably reflecting the contribution of fewer psychrotrophic and psychrotolerant taxa, as previously highlighted (De Filippis et al., 2013). Furthermore, seasonal differences in species richness were observed in the processing environment, with higher richness in summer. This pattern may be explained by differences in animal management, as summer cattle were outdoor-reared, likely carrying a broader environmental and soil-associated microbiome, whereas winter cattle were kept indoors, likely carrying a less diverse microbiome with stronger gut- and skin-associated signatures. These season-specific animal-associated microbiomes may have seeded the processing environment differently, contributing to higher richness from farm to upstream processing locations in summer while lower richness across the same stages in winter. Together, these findings suggest that seasonal differences at the animal level can propagate into the processing environment before the maturation stage, where temperature-controlled storage and packaging impose stronger selective pressure. Ultimately, this seasonal difference in microbiome composition was also reflected at the functional level, particularly through the higher spoilage-associated gene load observed in summer, while antimicrobial resistance, biocide resistance, and virulence-associated genes generally remained low or showed niche-specific patterns. These findings align with observations from poultry processing systems, where temperature-driven seasonal variation strongly shaped functional gene profiles (Baker et al., 2023).

Importantly, the presented data suggest that, besides food-contact surfaces, operators' hands and processing tools, such as knives, may represent important microbial transfer points across the processing chain. Indeed, the detection of spoilage-associated taxa and species potentially linked to food safety concerns, including *S. enterica*, on hands and knives in the Boning Hall suggests possible microbial transfer between operators, tools, and meat-contact materials. However, we have to point out that DNA extraction and sequencing cannot separate live

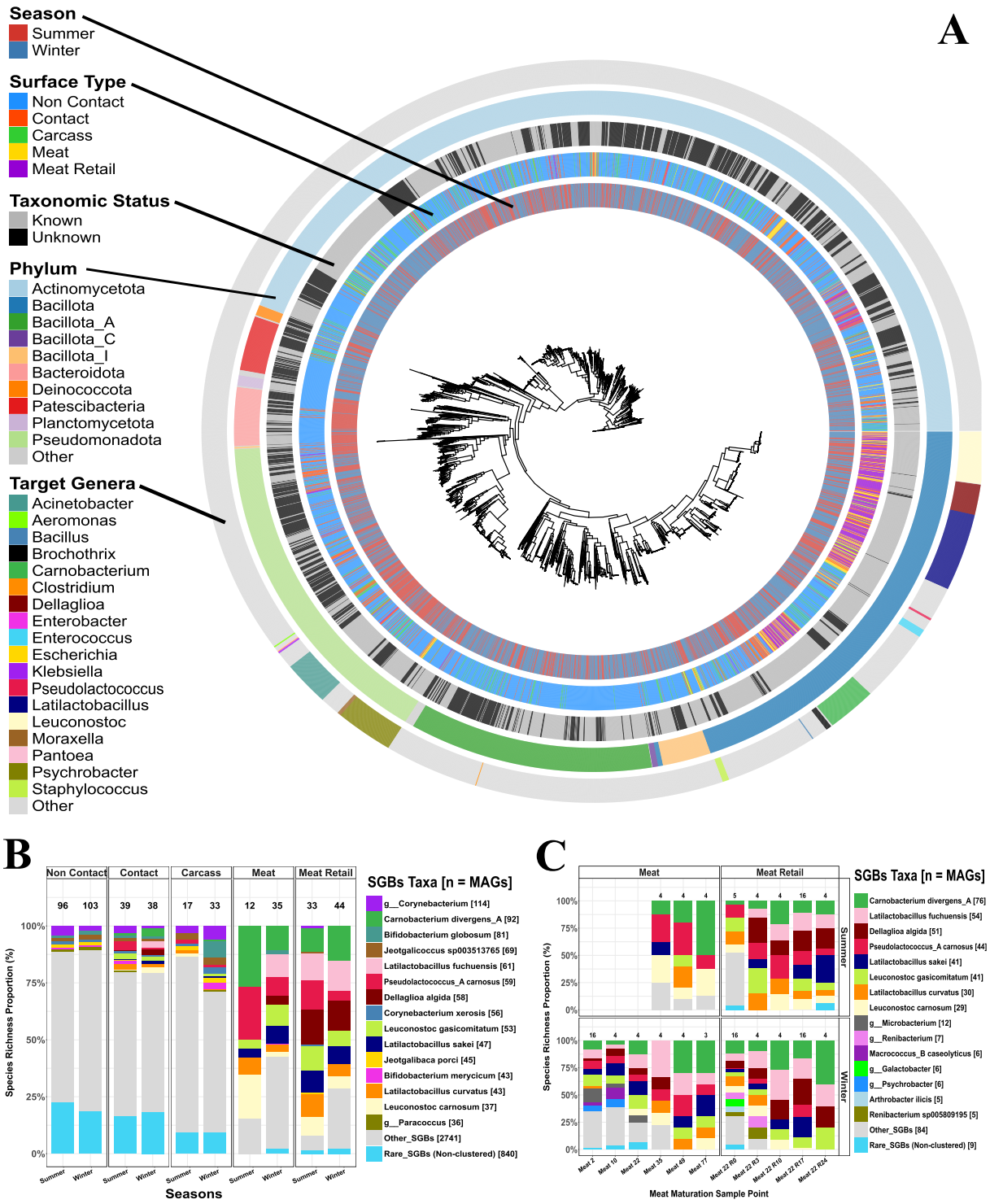

Fig. 6. (A) Phylogenomic tree of recovered medium/high-quality MAGs (n = 4475), showing their distribution across seasons, processing surfaces, and final meat products. For each MAG, rings indicate the season, processing surface-type, along with the known and unknown species-level assignment, phylum, and genus-level taxonomic classification from inner to outer rings. In the phylogenomic tree, the genus-level color ring highlights the 18 indicator genera that were successfully recovered as MAGs from the original list of 29 target genera. (B) Taxonomic distribution of genome-resolved groups across production surfaces and (C) during sequential meat maturation time points. Stacked bars represent the proportional distribution of unique SGBs per niche, with singleton SGBs and unassigned MAGs collapsed into the "Rare_SGBs" category for visualization. Total sample sizes (n) are indicated above each bar. Numbers in brackets in the legend denote the total number of MAGs assigned to each displayed SGB across the dataset. For "Rare_SGBs," the bracketed number represents the combined number of singleton-associated MAGs and unassigned MAGs.

cells from dead/inactive ones. Therefore, we cannot exclude that this pattern might represent trace of genetic material rather than an active hygiene failure. However, it does emphasize the importance of hygiene control and operator training. In addition, the hygiene control of materials used for vacuum-packaging of the meat is crucial, as the vacuum bags also contained detectable microbial communities that may contribute to contamination, as previously suggested (Zwirzitz et al., 2021).

Throughout the processing line, the meat microbiome undergoes dynamic changes. Indeed, the initial meat products harbor diverse microbial communities, likely reflecting early exposure to the processing environment, but maturation appears to impose a strong ecological filter, promoting the variety of a highly specialized, low-diversity microbial consortium, dominated by psychrotrophic LAB. Consistently, previous studies highlighted that vacuum packaging and low-temperature storage drive the meat community toward a psychrotrophic LAB-dominated consortium (Freitas et al., 2024; Pennacchia et al., 2011; Roch et al., 2025). In the present work, *C. divergens* and *C. maltaromaticum* were identified as key members of this consortium. These LAB species are frequently abundant in long-term, vacuum-packed meats (Leisner et al., 2007; Roch et al., 2025; T. Zhang et al., 2018). They may contribute to product stability through bacteriocin-associated genes with reported activity against L. *monocytogenes* (Martin-Visscher et al., 2011; P. Zhang et al., 2019; Evangelista et al., 2023; Andrade Cavalari et al., 2024), while also contributing to spoilage through proteolytic potential (Dallagnol et al., 2021; Quijada et al., 2022). Consistently, the enrichment of regulatory and protein metabolism pathways was observed in meat microbiomes during maturation, primarily driven by *Carnobacterium* species (Roch et al., 2025; Sequino et al., 2024). Interestingly, retail storage was associated with a further shift in meat microbiome composition, where the dominance of *Carnobacterium* spp. shifted toward *P. carnosus* and *P. paracarnosus*, potentially reflecting microbial inputs or selective pressures associated with slicing and portioning procedures during retail processing (Cauchie et al., 2020; Roch et al., 2025).

The detection of species potentially linked to food safety concerns, such as *S. enterica, L. monocytogenes, and S. aureus,* at very low mean relative abundances (<0.2% at the read level) throughout meat maturation may reflect the combined influence of vacuum packaging, low-temperature storage, LAB dominance, and the presence of predicted bacteriophages associated with these taxa. The dominance of LAB carrying bacteriocin-associated genes supports the possibility of bioprotective functional potential in matured meat, although antimicrobial activity was not directly measured in this study (Dallagnol et al., 2021; Fernandes et al., 2024; Gontijo et al., 2022; Koutsoumanis et al., 2024). In parallel, phage abundance showed a strong positive association with predicted bacterial host abundance, which is consistent with the Piggyback-the-Winner (PtW) hypothesis, where phages and bacterial hosts may coexist under specific ecological conditions (Silveira & Rohwer, 2016; Voigt et al., 2021). For example, biofilms can reduce phage diffusion and favor the replacement of susceptible host strains by resistant ones (Pires et al., 2021), resulting in the simultaneous survival of phages and hosts. However, localized negative associations between phages and predicted bacterial hosts were also observed in the present study. Higher predicted phage abundance coincided with lower relative abundance of L. *monocytogenes* in both the processing environment and meat products, while similar negative associations involving *S. aureus* and *S. enterica* were observed in meat products, which is consistent with the Kill-the-Winner (KtW) hypothesis. Overall, these patterns support the assumption that the resident phagome may contribute to microbial community structuring (Fernández-Gómez et al., 2025) and highlight the potential relevance of phages for biocontrol strategies in meat processing. However, these predictive associations should be interpreted cautiously, as metagenomic prediction and abundance modeling cannot directly demonstrate phage infection, host killing, or causal suppression.

Sanitation did not fully reshape the environmental microbiome across all sampled facilities, but it showed targeted effects on specific taxa. For instance, in the Retail Hall, sanitation reduced the relative abundance of some LAB species and *C. perfringens,* an anaerobic bacterium that can be associated with vacuum-packed meat products. However, several opportunistic and biofilm-forming taxa, including *A. baumannii* and *E. faecium,* remained detectable after cleaning. Because shotgun metagenomic sequencing does not distinguish viable from non-viable cells, these observations should be interpreted cautiously. The post-cleaning community profile may reflect multiple, non-mutually exclusive processes, including the removal of loosely attached bacteria and extracellular DNA during washing, persistence of DNA from inactivated cells protected within biofilm matrices, redistribution of microorganisms or DNA through aerosols generated during sanitation, and ecological shifts associated with the preferential removal of susceptible populations. Consequently, the detected post-cleaning taxa cannot be assumed to represent viable sanitizer-resistant populations. Nevertheless, previous studies have shown that exposure to sublethal concentrations of sanitizers can promote biofilm formation in surviving bacterial populations as an adaptive protective response (Cincarova et al., 2016; Slany et al., 2017). This interpretation is consistent with the functional data, where biofilm-associated genes showed a higher mean functional load in post-cleaning samples than in during-production samples, with only a modest increase in median load, although this difference was not statistically significant and showed high variability among post-cleaning samples. Therefore, the data do not support a uniform enrichment of biofilm genes after sanitation, but they do indicate that routine cleaning did not consistently reduce biofilm-related functional potential. This may reflect the greater tolerance of biofilm-associated cells compared with planktonic populations, as biofilms can facilitate persistence of taxa carrying biocide resistance, AMR, and virulence-associated genes (Fagerlund et al., 2021; Zwirzitz et al., 2020, Zwirzitz et al., 2021).

Genome-resolved reconstruction allowed the recovery of putative novel species-level lineages. The high number of singleton-associated and unclustered MAGs further indicates that the beef processing environment contains a large reservoir of rare or weakly connected lineages that are not well represented in current reference databases. Indeed, nearly 40% of reconstructed MAGs represented putative novel species, and their functional annotation suggests that some of these lineages may contribute to spoilage-associated potential. On the other hand, the environmental taxa identified as key functional reservoirs, including *Klebsiella grimontii, Aeromonas hydrophila, E. faecalis, Stenotrophomonas indicatrix,* and *Acinetobacter albensis,* were also recovered as MAGs across seasons, supporting their presence as recurrent community members rather than isolated read-level signals. Consistent with the low read-level abundance of several food safety-associated taxa, no MAGs assigned to major food safety-associated species, including *C. perfringens, K. pneumoniae, L. monocytogenes, S. enterica, Campylobacter jejuni,* and *Campylobacter coli,* were recovered from matured meat products. Thus, the lack of MAG recovery together with extremely low read-level abundance in matured meat products suggests that these persistent low-level detections did not represent stable, abundant members of the meat microbiome. Instead, they may reflect low-biomass carryover from the processing environment, transient contamination events, or taxa present below the coverage required for reliable MAG reconstruction, consistent with previous evidence that low-abundance microbial signals can be strongly influenced by background contamination in low-biomass datasets (Carini et al., 2016).

5. Conclusions

This farm-to-fork investigation reframes the beef processing chain as a dynamic microbial ecosystem. By tracing the same animals along the processing chain and sampling the same facilities across two seasons, this study provides an ecological description suggesting that seasonality, sanitation, and predicted phage-host associations may be linked with

microbiome shifts across the meat processing chain, highlighting the impact of environmental and processing selective pressures alongside putative phage-host interactions. We show that seasonality and animal herd management practices are major drivers of the initial microbiome structure, potentially influencing microbial responses to sanitation during processing. Furthermore, while initial microbial profiles varied by season, standardized maturation acted as a strong selective factor, promoting a more stable and specialized microbiome in final meat products. Although this study offers a high-resolution view of microbial succession, our results are based on DNA analysis; therefore, we cannot exclude that the detected microbial signals may originate from dead or metabolically inactive cells. Accordingly, the phage-microbiome interactions reported should be further experimentally validated and confirmed. However, with this limitation in mind, this work provides a comprehensive picture of microbiome evolution along the beef processing chain and supports a shift in meat science from the pursuit of sterility toward the management of safer, more sustainable, and ecologically balanced microbiome ecosystems.

CRediT authorship contribution statement

Asim ur Rahman: Writing – review & editing, Writing – original draft, Visualization, Methodology, Formal analysis, Data curation. **Vincenzo Valentino:** Writing – review & editing, Methodology, Investigation, Formal analysis. **José F. Cobo-Díaz:** Writing – review & editing, Methodology, Investigation, Data curation. **Giuseppina Sequino:** Writing – review & editing, Formal analysis. **Avelino Alvarez Ordóñez:** Writing – review & editing, Supervision, Resources. **Danilo Ercolini:** Writing – review & editing, Supervision, Resources, Project administration, Funding acquisition. **Francesca De Filippis:** Writing – review & editing, Writing – original draft, Supervision, Resources, Project administration, Funding acquisition, Conceptualization.

Declaration of competing interest

The authors declare that they have no known competing financial interests or personal relationships that could have appeared to influence the work reported in this paper.

Acknowledgements

AR is a PhD student of the CRESCENDO Doctorate Programme that received funding from the European Union Horizon 2020 research and innovation programme under the Marie Skłodowska-Curie programme (MSCA-COFUND-2020) with Grant Agreement No. 101034245.

Appendix A. Supplementary data

Supplementary data to this article can be found online at https://doi.org/10.1016/j.foodres.2026.119939.

Data availability

The raw shotgun metagenomic sequencing data generated in this study are publicly available in the NCBI Sequence Read Archive (SRA) under BioProject accession number PRJNA1233666

References

Alcock, B. P., Huynh, W., Chalil, R., Smith, K. W., Raphenya, A. R., Wlodarski, M. A., … McArthur, A. G. (2023). CARD 2023: Expanded curation, support for machine learning, and resistome prediction at the comprehensive antibiotic resistance database. *Nucleic Acids Research, 51*(D1), D690–D699. https://doi.org/10.1093/nar/gkac920

Almeida, A., Nayfach, S., Boland, M., Strozzi, F., Beracochea, M., Shi, Z. J., … Finn, R. D. (2021). A unified catalog of 204,938 reference genomes from the human gut microbiome. *Nature Biotechnology, 39*(1), 105–114. https://doi.org/10.1038/s41587-020-0603-3

Andrade Cavalari, C. M., Imazaki, P. H., Pirard, B., Lebrun, S., Vanleyssem, R., Gemmi, C., … de Macedo, R. E. F. (2024). *Carnobacterium maltaromaticum* as bioprotective culture against spoilage bacteria in ground meat and cooked ham. *Meat Science, 211*, Article 109441. https://doi.org/10.1016/j.meatsci.2024.109441

Baker, M., Zhang, X., Maciel-Guerra, A., Dong, Y., Wang, W., Hu, Y., Renney, D., Hu, Y., Liu, L., Li, H., Tong, Z., Zhang, M., Geng, Y., Zhao, L., Hao, Z., Senin, N., Chen, J., Peng, Z., Li, F., & Dottorini, T. (2023). Machine learning and metagenomics reveal shared antimicrobial resistance profiles across multiple chicken farms and abattoirs in China. *Nature Food, 4*(8), 707–720. https://doi.org/10.1038/s43016-023-00814-w

Barcenilla, C., Cobo-Díaz, J. F., De Filippis, F., Valentino, V., Cabrera Rubio, R., O'Neil, D., … Alvarez-Ordóñez, A. (2024). Improved sampling and DNA extraction procedures for microbiome analysis in food-processing environments. *Nature Protocols, 19*(5), 1291–1310. https://doi.org/10.1038/s41596-023-00949-x

Barcenilla, C., Cobo-Díaz, J. F., Puente, A., Valentino, V., De Filippis, F., Ercolini, D., … Alvarez-Ordóñez, A. (2024). In-depth characterization of food and environmental microbiomes across different meat processing plants. *Microbiome, 12*(1), 199. https://doi.org/10.1186/s40168-024-01856-3

Bates, D., Mächler, M., Bolker, B., & Walker, S. (2015). Fitting linear mixed-effects models using lme4. *Journal of Statistical Software, 67*(1), 1–48. https://doi.org/10.18637/jss.v067.i01

Benoit, G., Raguideau, S., James, R., et al. (2024). High-quality metagenome assembly from long accurate reads with metaMDBG. *Nature Biotechnology, 42*, 1378–1383. https://doi.org/10.1038/s41587-023-01983-6

Camacho, C., Coulouris, G., Avagyan, V., Ma, N., Papadopoulos, J., Bealer, K., & Madden, T. L. (2009). BLAST+: Architecture and applications. *BMC Bioinformatics, 10*(1), 421. https://doi.org/10.1186/1471-2105-10-421

Carini, P., Marsden, P. J., Leff, J. W., Morgan, E. E., Strickland, M. S., & Fierer, N. (2016). Relic DNA is abundant in soil and obscures estimates of soil microbial diversity. *Nature Microbiology, 2*, Article 16242. https://doi.org/10.1038/nmicrobiol.2016.242

Cauchie, E., Delhalle, L., Taminiau, B., Tahiri, A., Korsak, N., Burteau, S., … Daube, G. (2020). Assessment of spoilage bacterial communities in food wrap and modified atmospheres-packed minced pork meat samples by 16S rDNA metagenetic analysis. *Frontiers in Microbiology, 10*, 3074. https://doi.org/10.3389/fmicb.2019.03074

Chaumeil, P.-A., Mussig, A. J., Hugenholtz, P., & Parks, D. H. (2020). GTDB-Tk: A toolkit to classify genomes with the genome taxonomy database. *Bioinformatics, 36*(6), 1925–1927. https://doi.org/10.1093/bioinformatics/btz848

Chklovski, A., Parks, D. H., Woodcroft, B. J., & Tyson, G. W. (2023). CheckM2: A rapid, scalable and accurate tool for assessing microbial genome quality using machine learning. *Nature Methods, 20*(8), 1203–1212. https://doi.org/10.1038/s41592-023-01940-w

Cincarova, L., Polansky, O., Babak, V., Kulich, P., & Kralik, P. (2016). Changes in the expression of biofilm-associated surface proteins in *Staphylococcus aureus* food-environmental isolates subjected to sublethal concentrations of disinfectants. *BioMed Research International.* , Article 4034517. https://doi.org/10.1155/2016/4034517

Clarke, E., Sherrill-Mix, S., & Dawson, C. (2025). *ggbeeswarm: categorical scatter (violin point) plots*. https://doi.org/10.32614/CRAN.package.ggbeeswarm

Cobo-Díaz, J. F., Alvarez-Molina, A., Alexa, E. A., Walsh, C. J., Mencía-Ares, O., Puente-Gómez, P., … Alvarez-Ordóñez, A. (2021). Microbial colonization and resistome dynamics in food processing environments of a newly opened pork cutting industry during 1.5 years of activity. *Microbiome, 9*(1), 204. https://doi.org/10.1186/s40168-021-01131-9

Dallagnol, A. M., Pescuma, M., Espínola, N. G., Vera, M., & Vignolo, G. M. (2021). Hydrolysis of raw fish proteins extracts by *Carnobacterium maltaromaticum* strains isolated from Argentinean freshwater fish. *Biotechnology Reports, 29*, Article e00589. https://doi.org/10.1016/j.btre.2021.e00589

De Filippis, F., Storia, A. L., Villani, F., & Ercolini, D. (2013). Exploring the sources of bacterial spoilers in beefsteaks by culture-independent high-throughput sequencing. *PLoS One, 8*(7), Article e70222. https://doi.org/10.1371/journal.pone.0070222

De Filippis, F., Valentino, V., Alvarez-Ordóñez, A., Cotter, P. D., & Ercolini, D. (2021). Environmental microbiome mapping as a strategy to improve quality and safety in the food industry. *Current Opinion in Food Science, 38*, 168–176. https://doi.org/10.1016/j.cofs.2020.11.012

Evangelista, A. G., Danielski, G. M., Corrêa, J. A. F., Cavalari, C. M.d. A., Souza, I. R., Luciano, F. B., & Macedo, R. E. F.d. (2023). *Carnobacterium as a bioprotective and potential probiotic culture to improve food quality, food safety, and human health – A scoping review*. *Critical Reviews in Food Science and Nutrition, 63*(24), 6946–6959. https://doi.org/10.1080/10408398.2022.2038079

Fagerlund, A., Langsrud, S., & Møretrø, T. (2021). Microbial diversity and ecology of biofilms in food industry environments associated with *Listeria monocytogenes* persistence. *Current Opinion in Food Science, 37*, 171–178. https://doi.org/10.1016/j.cofs.2020.10.015

FAO. (2013). *Food wastage footprint: Impacts on natural resources summary report (Organisation des Nations Unies pour l'alimentation et l'agriculture)*. FAO. https://www.fao.org/4/i3347e/i3347e.pdf.

Fernandes, N., Achemchem, F., Gonzales-Barron, U., & Cadavez, V. (2024). Biopreservation strategies using bacteriocins to control meat spoilage and foodborne outbreaks. *Italian Journal of Food Safety, 13*(4), Article 12558. https://doi.org/10.4081/ijfs.2024.12558

Fernández-Gómez, P., Leong, D., Berg, G., Brennan, F., Caruso, T., Charles, T. C., … Cotter, P. D. (2025). Harnessing agri-food system microbiomes for sustainability and human health. *Frontiers in Science, 3*. https://doi.org/10.3389/fsci.2025.1575468

Fernández-Trapote, E., Cobo-Díaz, J. F., Oliveira, M., Puente, A., Berdejo, D., Puente, H., … Alvarez-Ordóñez, A. (2026). Microbiome and resistome successions in pig

carcasses and fresh pork meat throughout slaughtering, processing and shelf-life. *Microbiome, 14*(1), 67. https://doi.org/10.1186/s40168-025-02288-3
Freitas, C. F.d., Carvalho, L. M. V. F., Camargo, A. C., Almeida, O. G. G.d., Oliveira, R. R. d., De Martinis, E. P., … Nero, L. A. (2024). Bacterial microbiota shifts in vacuum-packed beef during storage at different temperatures: Impacts on blown pack spoilage. *Food Microbiology, 119,* Article 104448. https://doi.org/10.1016/j.fm.2023.104448
Gontijo, M. T. P., Ramia, N. E., Dijamentiuk, A., Elfassy, A., Taha, S., Mangavel, C., … Borges, F. (2022). Mining biosynthetic gene clusters in *Carnobacterium maltaromaticum* by interference competition network and genome analysis. *Microorganisms, 10*(9), 1794. https://doi.org/10.3390/microorganisms10091794
Jain, C., Rodriguez-R, L. M., Phillippy, A. M., Konstantinidis, K. T., & Aluru, S. (2018). High throughput ANI analysis of 90K prokaryotic genomes reveals clear species boundaries. *Nature Communications, 9*(1), 5114. https://doi.org/10.1038/s41467-018-07641-9
Kang, D. D., Li, F., Kirton, E., Thomas, A., Egan, R., An, H., & Wang, Z. (2019). MetaBAT 2: An adaptive binning algorithm for robust and efficient genome reconstruction from metagenome assemblies. *PeerJ, 7*, Article e7359. https://doi.org/10.7717/peerj.7359
Karwowska, M., Łaba, S., & Szczepański, K. (2021). Food loss and waste in meat sector—Why the consumption stage generates the most losses? *Sustainability, 13*(11), Article 11. https://doi.org/10.3390/su13116227
Kassambara, A. (2026). *ggpubr: "ggplot2" based publication ready plots*. https://doi.org/10.32614/CRAN.package.ggpubr
Kolde, R. (2025). *pheatmap: pretty heatmaps*. https://doi.org/10.32614/CRAN.package.pheatmap
Koutsoumanis, K., Allende, A., Bolton, D., Bover-Cid, S., Chemaly, M., De Cesare, A., … Alvarez-Ordóñez, A. (2024). Persistence of microbiological hazards in food and feed production and processing environments. *EFSA Journal, 22*(1), Article e8521. https://doi.org/10.2903/j.efsa.2024.8521
Kuznetsova, A., Brockhoff, P. B., & Christensen, R. H. B. (2017). lmerTest package: Tests in linear mixed effects models. *Journal of Statistical Software, 82*(13), 1–26. https://doi.org/10.18637/jss.v082.i13
Langmead, B. (2024). Kraken 2*, KrakenUniq and Bracken indexes.* [Computer software]. https://benlangmead.github.io/aws-indexes/k2.
Langmead, B., & Salzberg, S. L. (2012). Fast gapped-read alignment with bowtie 2. *Nature Methods, 9*(4), 357–359. https://doi.org/10.1038/nmeth.1923
Leisner, J. J., Laursen, B. G., Prévost, H., Drider, D., & Dalgaard, P. (2007). *Carnobacterium:* Positive and negative effects in the environment and in foods. *FEMS Microbiology Reviews, 31*(5), 592–613. https://doi.org/10.1111/j.1574-6976.2007.00080.x
Li, D., Liu, C.-M., Luo, R., Sadakane, K., & Lam, T.-W. (2015). MEGAHIT: An ultra-fast single-node solution for large and complex metagenomics assembly via succinct de Bruijn graph. *Bioinformatics, 31*(10), 1674–1676. https://doi.org/10.1093/bioinformatics/btv033
Liu, B., Zheng, D., Zhou, S., Chen, L., & Yang, J. (2022). VFDB 2022: A general classification scheme for bacterial virulence factors. *Nucleic Acids Research, 50*(D1), D912–D917. https://doi.org/10.1093/nar/gkab1107
Lu, J., Breitwieser, F. P., Thielen, P., & Salzberg, S. L. (2017). Bracken: Estimating species abundance in metagenomics data. *PeerJ Computer Science, 3*, Article e104. https://doi.org/10.7717/peerj-cs.104
Manfreda, C., Ghidini, S., Fuschi, A., Remondini, D., Guarneri, F., Alborali, G. L., … Ianieri, A. (2026). In-depth characterization of microbiome and resistome of carcasses and processing environments in a swine slaughterhouse. *Veterinary Microbiology, 312*, Article 110820. https://doi.org/10.1016/j.vetmic.2025.110820
Martin-Visscher, L. A., Yoganathan, S., Sit, C. S., Lohans, C. T., & Vederas, J. C. (2011). The activity of bacteriocins from *Carnobacterium maltaromaticum* UAL307 against gram-negative bacteria in combination with EDTA treatment. *FEMS Microbiology Letters, 317*(2), 152–159. https://doi.org/10.1111/j.1574-6968.2011.02223.x
Massicotte, P., & South, A. (2026). *rnaturalearth: world map data from natural earth*. https://doi.org/10.32614/CRAN.package.rnaturalearth
Nørrung, B., Andersen, J. K., & Buncic, S. (2009). Main concerns of pathogenic microorganisms in meat. In F. Toldrá (Ed.), *Safety of meat and processed meat* (pp. 3–29). Springer. https://doi.org/10.1007/978-0-387-89026-5_1.
Oksanen, J., Simpson, G. L., Blanchet, F. G., Kindt, R., Legendre, P., Minchin, P. R., … Weedon, J. (2026). *vegan: Community ecology package*. https://doi.org/10.32614/CRAN.package.vegan
Ondov, B. D., Treangen, T. J., Melsted, P., Mallonee, A. B., Bergman, N. H., Koren, S., & Phillippy, A. M. (2016). Mash: Fast genome and metagenome distance estimation using MinHash. *Genome Biology, 17*(1), 132. https://doi.org/10.1186/s13059-016-0997-x
Pal, C., Bengtsson-Palme, J., Rensing, C., Kristiansson, E., & Larsson, D. G. J. (2014). BacMet: Antibacterial biocide and metal resistance genes database. *Nucleic Acids Research, 42*(D1), D737–D743. https://doi.org/10.1093/nar/gkt1252
Palanisamy, V., Bosilevac, J. M., Barkhouse, D. A., Velez, S. E., & Chitlapilly Dass, S. (2023). Shotgun-metagenomics reveals a highly diverse and communal microbial network present in the drains of three beef-processing plants. *Frontiers in Cellular and Infection Microbiology, 13*. https://doi.org/10.3389/fcimb.2023.1240138
Pasolli, E., Asnicar, F., Manara, S., Zolfo, M., Karcher, N., Armanini, F., … Segata, N. (2019). Extensive unexplored human microbiome diversity revealed by over 150,000 genomes from metagenomes spanning age, geography, and lifestyle. *Cell, 176*(3), 649–662.e20. https://doi.org/10.1016/j.cell.2019.01.001
Pennacchia, C., Ercolini, D., & Villani, F. (2011). Spoilage-related microbiota associated with chilled beef stored in air or vacuum pack. *Food Microbiology, 28*(1), 84–93. https://doi.org/10.1016/j.fm.2010.08.010
Pires, D. P., Melo, L. D. R., & Azeredo, J. (2021). Understanding the complex phage-host interactions in biofilm communities. *Annual Review of Virology, 8*, 73–94. https://doi.org/10.1146/annurev-virology-091919-074222
Poore, J., & Nemecek, T. (2018). Reducing food's environmental impacts through producers and consumers. *Science, 360*(6392), 987–992. https://doi.org/10.1126/science.aaq0216
Quijada, N. M., Dzieciol, M., Schmitz-Esser, S., Wagner, M., & Selberherr, E. (2022). Metatranscriptomic analyses unravel dynamic changes in the microbial and metabolic transcriptional profiles in artisanal austrian hard-cheeses during ripening. *Frontiers in Microbiology, 13*, Article 813480. https://doi.org/10.3389/fmicb.2022.813480
R Core Team. (2024). *R: A language and environment for statistical computing [Computer software]*. R Foundation for Statistical Computing. https://www.r-project.org/.
Ramanathan, R., Lambert, L. H., Nair, M. N., Morgan, B., Feuz, R., Mafi, G., & Pfeiffer, M. (2022). Economic loss, amount of beef discarded, natural resources wastage, and environmental impact due to beef discoloration. *Meat and Muscle Biology, 6*(1), Article 1. https://doi.org/10.22175/mmb.13218
Richardson, C. (2026). ggforestplotR: Publication-ready forest plots with "ggplot2". https://github.com/thatoneguy006/ggforestplotR.
Roch, F.-F., Dzieciol, M., Strachan, C. R., Chaughtai, M. S., Quijada, N. M., Movsesijan, T., & Selberherr, E. (2025). Microbial succession and interaction in vacuum-packed beef: A longitudinal study of bacterial and fungal dynamics. *npj Science of Food, 9*(1), 105. https://doi.org/10.1038/s41538-025-00479-8
Schmieder, R., & Edwards, R. (2011). Quality control and preprocessing of metagenomic datasets. *Bioinformatics, 27*(6), 863–864. https://doi.org/10.1093/bioinformatics/btr026
Sequino, G., Cobo-Diaz, J. F., Valentino, V., Tassou, C., Volpe, S., Torrieri, E., … De Filippis, F. (2024). Microbiome mapping in beef processing reveals safety-relevant variations in microbial diversity and genomic features. *Food Research International (Ottawa, Ont.), 186*, Article 114318. https://doi.org/10.1016/j.foodres.2024.114318
Sequino, G., Cobo-Diaz, J. F., Valentino, V., Tassou, C., Volpe, S., Torrieri, E., … De Filippis, F. (2025). Environmental microbiome mapping in poultry processing chain and assessment of microbial dynamics in response to different storage conditions. *Food Microbiology, 128*, Article 104734. https://doi.org/10.1016/j.fm.2025.104734
Shang, J., Peng, C., Liao, H., Tang, X., & Sun, Y. (2023). PhaBOX: A web server for identifying and characterizing phage contigs in metagenomic data. *Bioinformatics Advances, 3*(1), Article vbad101. https://doi.org/10.1093/bioadv/vbad101
Shedleur-Bourguignon, F., Duchemin, T. P., Thériault, W., Longpré, J., Thibodeau, A., Hocine, M. N., & Fravalo, P. (2023). Distinct microbiotas are associated with different production lines in the cutting room of a swine slaughterhouse. *Microorganisms, 11*(1), Article 133. https://doi.org/10.3390/microorganisms11010133
Silveira, C. B., & Rohwer, F. L. (2016). Piggyback-the-winner in host-associated microbial communities. *npj Biofilms and Microbiomes, 2*(1), 16010. https://doi.org/10.1038/npjbiofilms.2016.10
Slany, M., Oppelt, J., & Cincarova, L. (2017). Formation of *Staphylococcus aureus* biofilm in the presence of sublethal concentrations of disinfectants studied via a transcriptomic analysis using transcriptome sequencing (RNA-seq). *Applied and Environmental Microbiology, 83*(24). https://doi.org/10.1128/AEM.01643-17. e01643-17.
South, A., Michael, S., & Massicotte, P. (2024). *rnaturalearthdata: world vector map data from natural earth used in "rnaturalearth"*. https://doi.org/10.32614/CRAN.package.rnaturalearthdata
The UniProt Consortium. (2025). UniProt: The universal protein knowledgebase in 2025. *Nucleic Acids Research, 53*(D1), D609–D617. https://doi.org/10.1093/nar/gkae1010
Véghová, A., Minarovičová, J., Koreňová, J., Drahovská, H., & Kaclíková, E. (2017). Prevalence and tracing of persistent *Listeria monocytogenes* strains in meat processing facility production chain. *Journal of Food Safety, 37*(2), Article e12315. https://doi.org/10.1111/jfs.12315
Voigt, E., Rall, B. C., Chatzinotas, A., Brose, U., & Rosenbaum, B. (2021). Phage strategies facilitate bacterial coexistence under environmental variability. *PeerJ, 9*, Article e12194. https://doi.org/10.7717/peerj.12194
Wheatley, P., Giotis, E. S., & McKevitt, A. I. (2014). Effects of slaughtering operations on carcass contamination in an Irish pork production plant. *Irish Veterinary Journal, 67*(1), 1. https://doi.org/10.1186/2046-0481-67-1
Wickham, H. (2016). *ggplot2: Elegant graphics for data analysis*. Springer-Verlag New York. https://ggplot2.tidyverse.org.
Wood, D. E., Lu, J., & Langmead, B. (2019). Improved metagenomic analysis with Kraken 2. *Genome Biology, 20*(1), 257. https://doi.org/10.1186/s13059-019-1891-0
World Wildlife Fund. (2021). *Driven to waste global food loss on farms* [Report Summary]. In *World Wildlife Fund; Driven to Waste: The Global Impact of Food Loss and Waste on Farms*. WWF. https://wwf.panda.org/discover/our_focus/food_practice/food_loss_and_waste/driven_to_waste_global_food_loss_on_farms.
Xu, Z. S., Pham, V. D., Yang, X., & Gänzle, M. G. (2025). High-throughput analysis of microbiomes in a meat processing facility: Are food processing facilities an establishment niche for persisting bacterial communities? *Microbiome, 13*(1), 25. https://doi.org/10.1186/s40168-024-02026-1
Yeom, J., Bae, D., & Kim, S. A. (2024). Microbial dynamics of South Korean beef and surroundings along the supply chain based on high-throughput sequencing. *Meat Science, 214*, Article 109520. https://doi.org/10.1016/j.meatsci.2024.109520
Yu, G., Smith, D., Zhu, H., Guan, Y., & Lam, T. T.-Y. (2017). Ggtree: An R package for visualization and annotation of phylogenetic trees with their covariates and other associated data. *Methods in Ecology and Evolution, 8*(1), 28–36. https://doi.org/10.1111/2041-210X.12628

Zhang, P., Gänzle, M., & Yang, X. (2019). Complementary antibacterial effects of bacteriocins and organic acids as revealed by comparative analysis of *Carnobacterium* spp. from meat. *Applied and Environmental Microbiology, 85*(20), Article e01227–19. https://doi.org/10.1128/AEM.01227-19

Zhang, T., Zhang, W., Ai, D., Zhang, R., Lu, Q., Luo, Q., & Shao, H. (2018). Prevalence and characterization of *Clostridium perfringens* in broiler chickens and retail chicken meat in Central China. *Anaerobe, MALDI-TOF MS in Anaerobe Diagnostics, 54*, 100–103. https://doi.org/10.1016/j.anaerobe.2018.08.007

Zhu, W., Lomsadze, A., & Borodovsky, M. (2010). Ab initio gene identification in metagenomic sequences. *Nucleic Acids Research, 38*(12), Article e132. https://doi.org/10.1093/nar/gkq275

Zwirzitz, B., Wetzels, S. U., Dixon, E. D., Fleischmann, S., Selberherr, E., Thalguter, S., … Stessl, B. (2021). Co-occurrence of *Listeria* spp. and spoilage associated microbiota during meat processing due to cross-contamination events. *Frontiers in Microbiology, 12*. https://doi.org/10.3389/fmicb.2021.632935

Zwirzitz, B., Wetzels, S. U., Dixon, E. D., Stessl, B., Zaiser, A., Rabanser, I., … Selberherr, E. (2020). The sources and transmission routes of microbial populations throughout a meat processing facility. *npj Biofilms and Microbiomes, 6*(1), 26. https://doi.org/10.1038/s41522-020-0136-z